PAGEOPH, Vol. 138, No. 1 (1992) 0033–4553/92/010043–18$1.50 + 0.20/0

One-station Estimates of Seismic Moments from the Mantle Magnitude M_m: The Case of the Regional Field ($1.5° \leq \Delta \leq 15°$)

JACQUES TALANDIER[1] and EMILE A. OKAL[2]

Abstract—We extend to the regional field of distances the procedure of one-station estimation of seismic moments using the mantle magnitude M_m, as introduced earlier in the case of teleseismic events. A theoretical analysis of the validity of the asymptotic expansion of normal modes in terms of surface waves, which was used in the development of M_m, upholds the validity of the algorithm for distances as short as 1.5°. This is confirmed by the analysis of a dataset of 149 GEOSCOPE records obtained at distances ranging from 1.5 to 15°, from earthquakes with moments between 10^{24} and 2.5×10^{27} dyn-cm. The performance of M_m as measured in terms of average residual with respect to published values of M_0, and standard deviation of the residuals, is not degraded in this distance range, with respect to the teleseismic case. This indicates that the mantle magnitude M_m can be reliably used at regional distances, notably for tsunami warning applications.

Key words: Mantle magnitude, tsunami warning, regional field.

1. Introduction and Purpose

The purpose of this paper is to test the variable-period mantle magnitude M_m in the case of regional epicentral distances, in practice $1.5° \leq \Delta \leq 15°$. The mantle magnitude M_m was introduced by OKAL and TALANDIER (1989; hereafter Paper I) as a convenient way of measuring in real time the seismic moment of a teleseismic event, while keeping the philosophy of a *magnitude* scale, i.e., a one-station estimate ignoring the exact depth and focal geometry of the source. The concept, initially developed on mantle Rayleigh waves, was later extended to Love waves (OKAL and TALANDIER, 1990; hereafter Paper II). The M_m algorithm has been successfully incorporated into a procedure of automatic event detection and quantification at teleseismic distances, which has measured more than 500 seismic moments in real time, since its implementation at the Geophysical Laboratory in Tahiti in 1987 (REYMOND *et al.*, 1991; HYVERNAUD *et al.*, 1992).

[1] Laboratoire de Détection et Géophysique and Centre Polynésien de Prévention des Tsunamis, Commissariat à l'Energie Atomique, Boîte Postale 640, Papeete, Tahiti, French Polynesia.

[2] Department of Geological Sciences, Northwestern University, Evanston, Illinois 60208, U.S.A.

Our previous studies were concerned with the general features of the magnitude M_m, and their datasets emphasized teleseismic distances. Given the potential of the method in the field of tsunami warning (TALANDIER and OKAL, 1989), it is particularly important to assess its performance at regional distances for which the ability to obtain real-time estimates of the size of an earthquake becomes crucial. In Papers I and II, we did verify that the quality of moment determinations was not lessened when restricted to the shortest paths then available. Such tests were, however, limited to small datasets of only a few points, with no distances smaller than 7.3 degrees.

With the development of broadband networks, notably the implementation of GEOSCOPE stations in the immediate vicinity of subduction zones, it recently became possible to acquire a much larger set of high quality data covering the whole range of regional distances. Also, our experience in Papeete, Tahiti shows that accurate measurements can be obtained routinely down to $M_m = 4$ (or $M_0 = 10^{24}$ dyn-cm) (REYMOND *et al.*, 1991). This opens the way for a much more systematic investigation of the performance of M_m at regional distances, which is the subject of the present paper.

We will see that in practice measurements can be taken for any distance $\Delta \geq 1.5°$. This lower bound of distances is predicted by an examination of the breakdown of the asymptotic expansion of Legendre polynomials used in the development of the M_m algorithm. At even shorter distances, the seismogram is dominated by near field terms. A procedure to extend the concept of M_m to the near field will be the subject of a separate paper.

The present study involves only Rayleigh waves recorded on vertical seismograms; since it follows closely the work reported in Paper I, we will emphasize only those aspects specifically related to the issue of short distances. We simply recall that the mantle magnitude M_m is obtained from the spectrum of mantle Rayleigh waves through:

$$M_m = \log_{10} X(\omega) + C_S + C_D - 0.90 \tag{1}$$

where $X(\omega)$ is the spectral amplitude in μm-s at the angular frequency ω. The expressions for the frequency-dependent distance and source corrections C_D and C_S are given in Paper I. The measurements are carried out at all Fourier periods between 50 and 300 s, and the largest number retained. Its value is then expected to represent $[\log_{10} M_0 - 20]$, where M_0 is measured in dyn-cm. In practice, and based on a dataset of several hundred measurements, the precision achieved at teleseismic distances is on the order of 0.2 units of magnitude.

From the theoretical standpoint, there are two reasons to expect the breakdown of the M_m formalism at short distances: in the first place, the source and distance corrections in (1) are based on the asymptotic expansion of the Legendre polynomials,

$$P_l^m(\cos\Delta) = (-1)^m l^{m-1/2} \sqrt{\frac{2}{\pi \sin\Delta}} \cdot \cos\left[(l+\tfrac{1}{2})\Delta + m\frac{\pi}{2} - \frac{\pi}{4}\right] \tag{2}$$

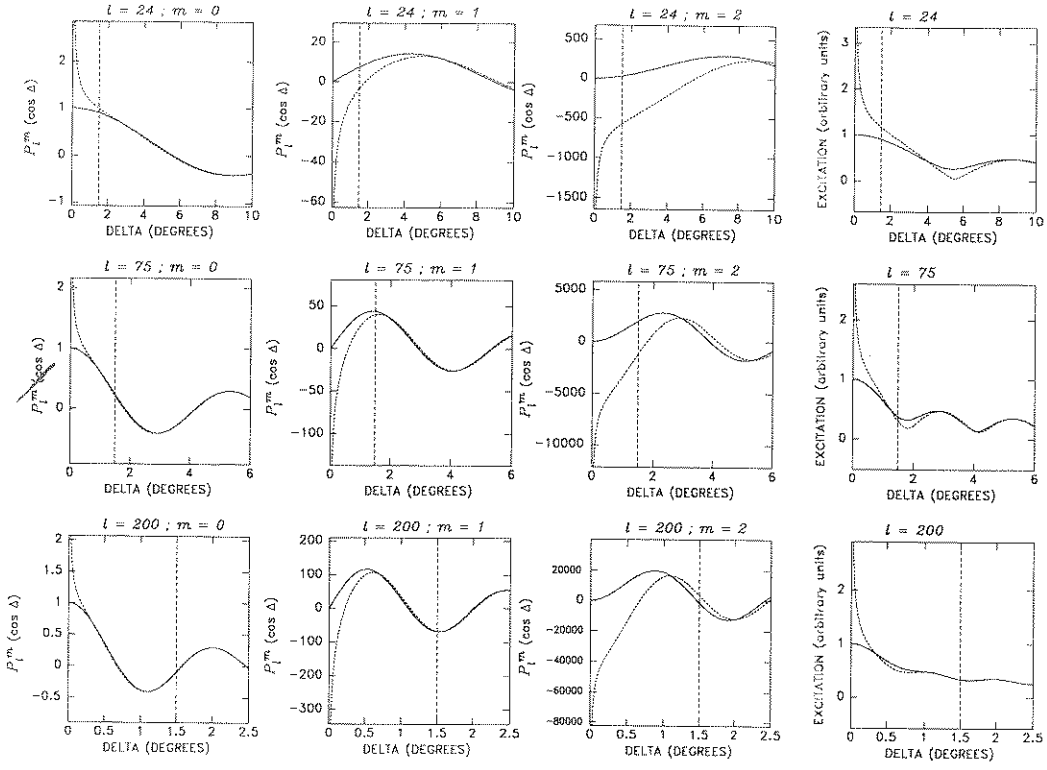

Figure 1

Deterioration of the asymptotic expansion of P_l^m as a function of distance, for values of l representative of mantle waves. On each row, the left three plots compare the true value of P_l^m, computed by recurrence on l (solid line), to the expression derived from the asymptotic expansion (dotted line). The fourth box similarly compares the average excitation $\langle Ex \rangle$ (Equation 3) computed by both algorithms. In all cases, the vertical dashed line shows the lower bound of the range of distances in our dataset ($\Delta = 1.5°$).

which diverges like $1/\sqrt{\sin \Delta}$ as $\Delta \to 0$; in addition, our formalism, developed at teleseismic distances, neglects the near-field terms, whose contribution to spectral amplitudes becomes prominent at very short distances. These effects will be studied in detail in a separate paper, but it is at least possible to discuss in general terms the breakdown of the asymptotic expansion.

In order to put some theoretical bounds on the possible range of the asymptotic breakdown, we proceed as follows. In Figure 1, we study the deterioration of the asymptotic approximation at three angular orders ($l = 24$, 75 and 200) representative of mantle Rayleigh waves (the corresponding periods would be close to 300, 125 and 50 s, respectively). On each row of plots, the first three boxes show the variation of P_l^m with distance in the range of a few degrees, for the three degrees ($m = 0$, 1, 2) excited by a double-couple. The solid lines are the exact values of P_l^m,

computed by recurrence over l, and the dotted lines the values computed by using (2). As expected, the latter diverge significantly in the vicinity of $\Delta = 0$. The vertical dashed line marks $\Delta = 1.5°$, the limit of our available data (see below). While the P_l^0 are in all cases fit correctly by the asymptotic expansion, the figure suggests that the M_m algorithm could be invalid at distances shorter than 7° for the lowest frequencies considered, due a significant misfit of P_{24}^2 when using (2). However, when considering the full Rayleigh excitation, in the notation of KANAMORI and CIPAR (1974).

$$Ex = |s_R K_0 P_l^0 - q_R K_1 P_l^1 + p_R K_2 P_l^2| \tag{3}$$

the situation is made more subtle by the relative amplitudes of the excitation coefficients K_i. (Note that Ex is the normal mode equivalent to the excitation E defined in Equation (8) of Paper I, using the surface wave formalism. As such, it remains a function of distance: in the normal mode formalism excitation and propagation do not separate.) Following the approach in Paper I, we computed the average $\langle Ex \rangle$, over a large number of source-receiver geometries, both using the exact values of the P_l^m, and the asymptotic expansion (2), for a source at 20 km depth. Results are shown in the three boxes at far right on Figure 1. It is clear that the error introduced by using the asymptotic expansion has been reduced considerably, through the weighting of P_l^m by the K_m, to the point where it remains less than 50% (or 0.3 units of magnitude) for $\Delta \geq 1.5°$. It must be borne in mind that the above argument involves an average focal mechanism, and would not hold for all source-receiver geometries. Nevertheless, in keeping with the general concept of magnitude, we would expect that the deterioration of the asymptotic expansion of the P_l^m polynomials should not affect significantly the validity of Equation (1) as far as estimating the mantle magnitude M_m, at distances as short as 1.5° and for all periods $T \leq 300$ s.

2. Dataset

In order to gather an adequate dataset, we searched systematically the Harvard CMT solutions (DZIEWONSKI *et al.*, 1983a; and subsequent updates) for events with moments greater than 10^{24} dyn-cm, having taken place within 15° of a GEOSCOPE station. The threshold of 10^{24} dyn-cm is in line with our observation (REYMOND *et al.*, 1991) that such moments are accurately recovered at teleseismic distances through the M_m algorithm. In selecting the events, we tried to obtain a balanced coverage through the moment range. In this respect, we generally selected all events with $M_0 > 10^{25}$ dyn-cm, but kept only a representative number in the range 10^{24}–10^{25}, as the population of such events would have become prohibitively large for stations close to subduction zones, especially during aftershock sequences.

M_m: Map of Regional Dataset

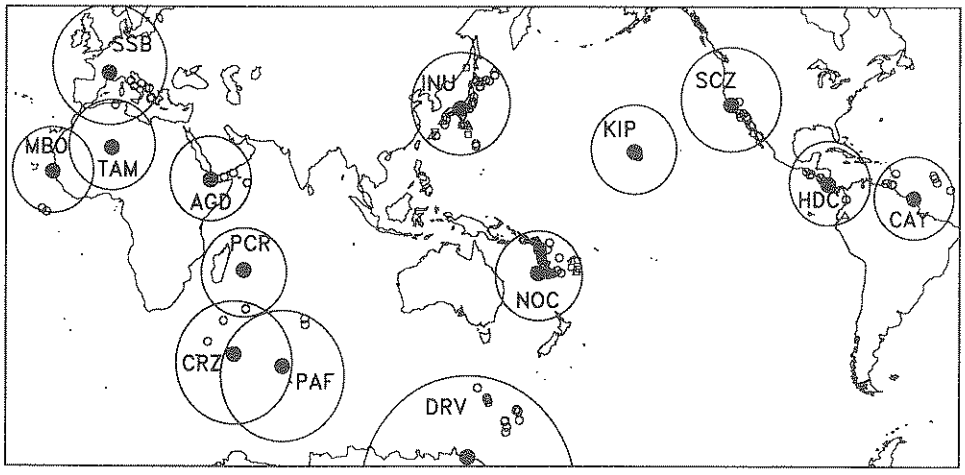

Figure 2
Map of the dataset used in this study. The loops are small circles delineating 15° of distance around each GEOSCOPE station. Inside each loop, events are plotted according to the following key: circles: shallow ($h \leq 75$ km); upward-pointing triangles: intermediate (A) ($h = 75$–200 km); downward triangles: intermediate (B) ($h = 200$–400 km); squares: deep ($h \geq 400$ km).

This search resulted in 149 records; not surprisingly, the two stations at Inuyama, Japan (INU) and Nouméa, New Caledonia (NOC, later moved to NOU, 24 km to the NW), both located in the immediate vicinity of subduction zones, provided the bulk of the data. The epicentral distances range from 1.51° (04 September 1988 recorded at INU) to 14.73° (07 June 1987 at M'Bour, Sénégal), and the moments from 10^{24} dyn-cm (03 May 1987 at INU) to 2.5×10^{27} dyn-cm (10 August 1988 at NOU). Both shallow and intermediate and deep events were analyzed, the maximum depth being 623 km. The geographical distribution of events is shown on Figure 2, and Table 1 summarizes all pertinent epicentral information as obtained from the Harvard files. Figure 3 further shows that, even though the largest event in the dataset correpsonds to a relatively large distance (12.99°), there is no systematic correlation between distance and moment, with a few significantly large earthquakes recorded at some of the shortest distances (e.g., the 15 January 1986 event (4.6×10^{26} dyn-cm) at NOC; $\Delta = 3.69°$). As such, our conclusions on the performance of M_m in the regional field will not be biased by the absence of large sources at the shortest distances.

Table 1

Dataset and Results of the Present Study

Date D M Y	Epicenter (°N; °E)	Depth (km)	M_m^{pub}	Focal Solution (ϕ, δ, λ)	Ref. †	Station	Δ (°)	M_m	Period (s)	M_c
				Shallow Events						
9 1 1983	38.17 20.23	15	4.76	57 35 -168	a	SSB	13.69	4.28	98.46	4.7
23 3 1983	38.33 20.22	33	5.34	27 59 175	a	SSB	13.59	5.01	64.00	5.41
24 3 1983	38.18 20.32	25	4.15	65 56 -156	a	SSB	13.74	3.84	67.37	4.06
14 5 1983	38.49 20.36	15	4.15	119 82 8	b	SSB	13.59	4.29	106.67	4.58
29 4 1984	43.27 12.57	10	4.53	143 21 -72	c	SSB	6.11	4.52	182.86	4.65
7 5 1984	41.77 13.89	10	4.89	174 31 -52	c	SSB	7.65	5.04	256.00	4.98
2 7 1985	-33.85 56.35	10	4.48	110 46 -59	d	PCR	12.64	5.20	160.00	4.67
2 7 1985	-33.80 56.43	10	4.89	109 44 -63	d	PCR	12.60	5.62	116.36	5.08
22 9 1985	12.49 -44.33	10	4.69	196 31 111	d	CAY	10.90	5.15	80.00	4.88
27 10 1985	36.40 6.75	10	4.79	213 71 20	e	SSB	9.03	5.41	75.29	4.94
27 10 1985	36.40 6.75	10	4.79	213 71 20	e	TAM	13.63	5.39	67.37	5.00
16 12 1985	-14.15 166.36	32	5.81	166 46 -122	e	NOC	8.11	5.50	91.43	5.88
21 12 1985	-14.04 166.51	46	6.76	165 44 88	e	NOC	8.22	6.67	182.86	6.61
21 12 1985	-14.19 166.71	50	5.85	179 42 99	e	NOC	8.08	5.62	160.00	5.72
21 12 1985	-14.48 166.79	38	5.46	17 45 123	e	NOC	7.79	5.32	160.00	5.80
24 12 1985	-14.20 166.31	33	4.72	337 44 87	e	NOC	8.06	4.99	80.00	5.03
25 12 1985	-13.91 169.91	28	4.74	282 67 -7	e	NOC	8.98	4.78	71.11	5.15
28 12 1985	-13.19 166.57	44	5.51	160 45 76	e	NOC	9.07	5.32	160.00	5.73
22 1 1986	-10.19 161.06	69	5.45	116 38 64	f	NOC	13.11	5.41	80.00	5.57
27 1 1986	-10.40 161.18	37	5.06	162 30 162	f	NOC	12.87	5.43	71.11	5.27
2 2 1986	-13.62 166.61	58	4.95	184 40 92	f	NOC	8.64	4.88	160.00	5.33
24 2 1986	-16.91 174.29	15	4.95	274 45 -20	f	NOC	9.14	5.11	106.67	5.10
1 3 1986	-62.80 154.49	15	4.79	330 73 -15	f	DRV	7.28	4.90	160.00	4.83
14 4 1986	-13.95 166.98	44	5.48	160 42 82	g	NOC	8.33	5.35	160.00	5.66
1 5 1986	-21.92 170.33	44	5.20	357 53 175	g	NOC	3.63	5.03	128.00	5.63
19 5 1986	-12.73 167.31	15	4.82	205 32 -99	g	NOC	9.56	5.05	64.00	5.12
23 5 1986	12.66 48.11	15	4.65	314 44 -62	g	AGD	5.29	5.07	106.67	4.86
31 5 1986	-57.32 147.71	15	4.38	165 86 2	g	DRV	10.02	4.93	91.43	4.52
11 6 1986	10.60 -62.95	20	5.46	97 52 -161	g	CAY	11.94	5.76	64.00	5.72
5 7 1986	-60.79 154.17	15	5.15	156 75 -12	h	DRV	8.58	5.54	256.00	5.22
7 7 1986	10.42 56.76	15	5.60	242 42 98	h	AGD	13.73	5.98	256.00	5.67
8 7 1986	34.00 -116.61	15	5.13	294 37 156	h	SCZ	4.70	5.21	91.43	5.20
13 7 1986	33.02 -117.79	15	4.81	126 37 106	h	SCZ	4.65	4.97	256.00	4.79
20 7 1986	37.58 -118.45	15	4.75	223 54 -35	h	SCZ	2.55	5.26	64.00	4.89
21 7 1986	37.54 -118.45	15	5.43	149 60 -163	h	SCZ	2.54	5.88	64.00	5.62
23 7 1986	-61.93 154.78	15	4.89	334 84 -5	h	DRV	7.95	5.11	128.00	4.93
17 9 1986	10.52 56.91	15	5.36	126 81 -179	h	AGD	13.87	5.62	91.43	5.24
23 9 1986	-16.59 167.23	15	4.92	271 75 4	h	NOC	5.73	4.66	64.00	4.87
14 10 1986	-43.21 41.99	15	5.30	99 84 0	i	CRZ	7.71	5.65	75.29	5.40
23 10 1986	-10.98 165.17	15	6.15	332 15 97	i	NOC	11.34	6.13	213.33	6.32
23 10 1986	-11.08 165.52	15	5.76	348 14 112	i	NOC	11.21	5.57	160.00	5.94
24 10 1986	-10.96 164.98	15	5.07	203 28 -42	i	NOC	11.38	4.86	91.43	4.97
24 10 1986	-10.86 165.22	15	5.46	354 16 114	i	NOC	11.45	5.29	80.00	5.73
25 10 1986	-17.62 168.12	45	5.32	164 45 80	i	NOC	4.92	5.37	213.33	5.42
1 12 1986	-56.83 147.32	15	4.84	166 69 -6	i	DRV	10.43	5.38	85.33	5.00
13 12 1986	-17.91 167.55	15	4.71	356 31 158	i	NOC	4.49	4.87	128.00	4.87
26 12 1986	-54.29 143.73	15	4.82	353 78 -9	i	DRV	12.53	5.02	106.67	4.91
28 12 1986	-38.40 78.93	15	5.45	223 70 -7	i	PAF	12.61	5.68	106.67	5.58
3 1 1987	-14.99 167.92	17	6.08	158 32 74	j	NOC	7.41	6.25	213.33	6.24
4 2 1987	19.79 -156.49	15	4.23	266 33 23	j	KIP	2.17	4.57	160.00	5.11

Table 1 (continued)

Date D M Y	Epicenter (°N; °E)	Depth (km)	M_m^{pub}	Focal Solution (ϕ, δ, λ)	Ref. †	Station	Δ (°)	M_m	Period (s)	M_c
7 2 1987	-59.14 159.07	15	4.45	264 78 4	j	DRV	11.43	4.96	106.67	4.53
7 2 1987	32.39 -115.39	15	4.32	202 70 2	j	SCZ	6.50	4.61	160.00	4.38
11 2 1987	-15.82 167.26	33	5.68	315 40 62	j	NOC	6.49	5.80	160.00	5.83
17 2 1987	-19.71 168.73	22	4.66	258 30 -93	j	NOC	3.35	4.93	160.00	4.81
27 2 1987	38.50 20.26	15	4.66	46 37 -155	j	SSB	13.52	4.92	213.33	4.97
18 3 1987	31.97 131.70	38	6.07	348 27 -103	j	INU	5.58	6.24	142.22	6.15
7 4 1987	37.35 141.68	31	6.06	203 16 88	k	INU	4.25	6.11	64.00	6.10
16 4 1987	-22.30 171.81	15	4.87	72 67 -10	k	NOC	4.98	5.06	91.43	5.11
21 4 1987	-22.79 170.17	15	5.23	104 40 -105	k	NOC	3.49	5.37	256.00	5.48
11 5 1987	38.82 141.96	43	4.81	202 25 93	k	INU	5.24	4.76	64.00	4.78
7 6 1987	-0.22 -19.19	15	4.76	79 85 -179	k	MBO	14.73	4.86	106.67	4.62
24 6 1987	-21.25 173.57	30	5.75	294 89 180	k	NOC	6.71	6.22	128.00	6.03
26 6 1987	-21.30 169.20	17	5.20	354 31 114	k	NOC	2.75	5.66	80.00	5.49
6 7 1987	-14.12 167.86	15	6.00	159 42 84	l	NOC	8.25	6.29	67.37	7.84
8 8 1987	-58.67 158.48	15	4.52	241 71 -4	l	DRV	11.60	4.96	91.43	4.70
12 8 1987	14.11 -59.26	15	4.54	152 90 180	l	CAY	11.41	4.71	213.33	5.02
3 9 1987	-58.90 158.30	15	7.15	155 69 -172	l	DRV	11.36	7.55	213.33	7.47
24 9 1987	36.53 141.20	20	4.89	217 14 106	l	INU	3.58	4.90	64.00	4.70
1 10 1987	34.05 -118.08	15	4.93	270 31 98	m	SCZ	3.72	5.12	106.67	4.80
6 11 1987	43.43 146.28	62	4.15	235 39 133	m	INU	10.78	4.42	64.00	4.27
17 11 1987	12.57 -86.98	56	5.76	264 17 51	m	HDC	3.80	5.36	64.00	5.87
19 11 1987	24.23 142.61	30	4.67	157 20 86	m	INU	12.11	4.36	80.00	5.15
24 11 1987	33.08 -115.78	15	5.15	305 90 180	m	SCZ	5.80	4.97	213.33	5.43
24 11 1987	33.01 -115.85	15	5.86	133 78 178	m	SCZ	5.80	5.79	64.00	7.83
15 12 1987	23.41 142.87	45	4.99	146 29 81	m	INU	12.95	4.72	213.33	5.46
17 12 1987	35.35 140.26	21	5.85	76 41 2	m	INU	2.64	5.91	64.00	5.59
9 1 1988	41.24 19.60	15	4.95	321 12 62	n	SSB	11.70	4.87	256.00	5.05
24 1 1988	26.73 128.05	44	4.80	299 51 49	n	INU	11.54	5.19	256.00	4.89
12 2 1988	30.13 -113.97	15	4.73	127 72 -177	n	SCZ	9.00	4.84	80.00	4.85
23 2 1988	-60.68 159.48	15	4.97	175 80 -172	n	DRV	10.46	5.50	213.33	5.15
26 2 1988	-37.30 47.97	15	6.26	318 33 89	n	CRZ	9.57	6.72	213.33	6.58
10 3 1988	10.36 -60.58	54	6.04	256 38 -67	n	CAY	9.80	6.46	213.33	6.31
12 3 1988	10.16 -60.59	33	4.79	42 31 -133	n	CAY	9.70	5.05	160.00	4.95
16 3 1988	10.27 -60.62	55	4.66	40 45 -118	n	CAY	9.79	5.20	182.86	5.10
23 3 1988	10.90 -43.56	15	5.30	178 71 -1	n	CAY	10.51	5.81	213.33	5.48
4 4 1988	30.39 131.21	42	4.98	163 27 30	o	INU	6.96	4.51	256.00	5.06
26 4 1988	42.37 16.57	15	4.15	289 44 121	o	SSB	9.17	4.55	256.00	4.65
3 5 1988	-22.81 170.25	15	5.15	129 30 -68	o	NOU	3.72	5.39	213.33	5.57
7 5 1988	43.28 147.83	15	4.26	222 23 101	o	INU	11.51	4.65	256.00	4.63
16 5 1988	-13.91 166.24	42	5.08	180 30 -115	o	NOU	8.17	4.89	182.86	5.24
17 5 1988	-11.50 170.67	15	5.34	248 59 -27	o	NOU	11.37	5.27	64.00	5.14
18 5 1988	38.42 20.47	23	4.04	163 38 95	o	SSB	13.70	4.70	213.33	4.57
18 5 1988	13.51 -44.85	15	4.75	348 43 -111	o	CAY	11.27	5.18	213.33	4.90
20 5 1988	8.10 -38.37	15	5.08	178 82 8	o	CAY	14.21	5.31	213.33	5.47
18 6 1988	13.58 -91.12	15	4.65	268 18 56	o	HDC	7.72	4.74	213.33	5.49
18 6 1988	26.92 -110.94	15	6.04	38 78 -10	o	SCZ	13.12	6.13	256.00	6.28
24 6 1988	10.23 -60.60	53	4.88	238 44 -89	o	CAY	9.80	5.40	213.33	5.18
28 6 1988	-56.41 147.15	15	5.08	78 74 174	o	DRV	10.81	5.60	91.43	5.30
6 7 1988	41.77 144.32	36	5.40	232 21 118	p	INU	8.58	4.97	213.33	5.43
6 7 1988	41.68 144.19	15	4.36	67 50 126	p	INU	8.45	3.96	213.33	4.02
16 7 1988	13.99 51.63	15	4.49	28 76 175	p	AGD	8.94	5.01	213.33	4.61
30 7 1988	44.78 149.85	51	4.70	183 39 28	p	INU	13.58	4.65	64.00	4.59
31 7 1988	-22.25 171.03	52	5.91	94 70 10	p	NOU	4.22	6.05	64.00	6.12

Table 1 (continued)

Date D M Y	Epicenter (°N; °E)	Depth (km)	M_m^{pub}	Focal Solution (ϕ, δ, λ)	Ref. †	Station	Δ (°)	M_m	Period (s)	M_c
10 8 1988	-10.21 160.77	16	7.40	346 19 116	p	NOU	12.99	7.27	256.00	7.67
16 8 1988	-36.74 78.79	15	4.36	138 90 180	p	PAF	14.06	4.85	213.33	4.58
27 8 1988	0.89 -20.99	15	4.30	255 73 -175	p	MBO	14.03	4.47	213.33	4.12
4 9 1988	35.38 138.88	31	4.08	163 36 12	p	INU	1.51	4.44	213.33	4.45
8 9 1988	-60.93 154.05	15	4.95	156 71 4	p	DRV	8.43	5.40	213.33	5.20
11 9 1988	14.66 -92.59	49	4.36	82 36 -146	p	HDC	10.03	4.47	160.00	4.74
20 9 1988	4.68 -77.43	24	4.82	14 18 104	p	HDC	8.51	5.15	256.00	5.05
2 11 1988	-56.85 147.45	15	4.67	261 90 180	q	DRV	10.43	5.27	85.33	4.93
3 11 1988	13.82 -90.61	54	5.95	96 10 -127	q	HDC	7.39	5.89	80.00	6.07
5 11 1988	-22.01 170.04	34	5.30	313 32 83	q	NOU	3.47	5.59	98.46	5.53
6 11 1988	-21.97 170.03	37	4.61	327 35 115	q	NOU	3.46	4.75	98.46	4.79
7 11 1988	-22.20 174.95	15	6.26	235 26 10	q	NOU	8.01	6.26	64.00	6.19
				Intermediate (A) Events						
15 1 1986	-21.38 170.28	121	6.66	17 28 164	f	NOC	3.69	6.96	160.00	6.89
22 10 1986	-10.63 166.03	183	5.03	341 23 68	i	NOC	11.63	5.10	160.00	5.25
23 10 1986	-15.56 167.64	171	5.41	312 59 4	i	NOC	6.80	5.42	160.00	5.55
26 3 1987	-13.72 167.18	194	5.32	336 38 89	j	NOC	8.57	5.25	91.43	5.37
18 6 1987	-10.69 162.19	86	5.57	310 51 174	k	NOC	12.25	5.77	213.33	5.73
3 7 1987	31.19 130.32	167	4.78	239 6 144	l	INU	6.98	4.94	160.00	4.72
12 8 1987	-12.26 166.64	104	4.89	34 68 -21	l	NOC	10.00	5.19	213.33	5.20
14 9 1987	30.49 139.67	167	4.52	122 27 -170	l	INU	5.34	4.73	213.33	4.48
23 9 1987	46.01 149.51	131	4.76	323 67 -21	l	INU	14.23	4.53	213.33	4.88
12 12 1987	29.68 140.04	166	5.56	103 53 -148	m	INU	6.20	5.70	213.33	5.61
2 1 1988	43.32 142.42	180	4.94	36 11 -146	n	INU	8.99	5.31	256.00	4.93
6 5 1988	11.46 -85.93	76	6.00	212 18 -29	o	HDC	2.28	5.97	91.43	6.17
7 5 1988	42.61 143.72	89	4.92	207 6 8	o	INU	8.92	5.11	91.43	4.88
2 7 1988	-14.30 167.19	148	5.53	191 47 112	p	NOU	7.83	5.51	91.43	6.24
27 7 1988	-13.16 167.06	183	6.11	180 48 118	p	NOU	8.95	6.20	98.46	6.30
27 7 1988	-13.14 166.96	176	4.99	175 42 133	p	NOU	8.96	5.19	256.00	4.99
10 8 1988	-14.88 167.30	142	6.21	179 51 147	p	NOU	7.26	6.44	91.43	6.46
15 9 1988	-1.41 -77.87	169	5.36	121 28 -109	p	HDC	12.99	5.34	160.00	5.47
7 11 1988	26.52 126.39	114	4.96	55 10 95	q	INU	12.68	4.45	91.43	4.96
				Intermediate (B) Events						
5 3 1986	-18.80 169.58	292	5.20	73 59 150	f	NOC	4.56	5.22	213.33	5.27
23 2 1987	-15.82 167.87	225	6.46	165 48 165	j	NOC	6.59	6.56	142.22	6.45
3 5 1987	28.47 127.58	208	4.00	16 11 10	k	INU	10.56	4.16	160.00	3.99
16 7 1987	32.99 138.00	301	4.88	54 30 147	l	INU	2.49	4.85	213.33	5.12
12 10 1987	32.50 137.77	352	4.18	87 33 154	m	INU	2.91	4.08	160.00	4.20
				Deep Events						
26 5 1986	-21.72 -179.26	603	6.32	60 59 -149	g	NOC	13.28	6.07	213.33	6.25
26 5 1986	-20.07 178.72	568	6.75	197 21 -176	g	NOC	11.67	6.61	213.33	6.80
7 5 1987	46.77 139.21	442	6.26	51 38 146	k	INU	11.53	6.06	213.33	6.05
26 8 1987	-20.78 -178.50	588	5.26	129 17 -170	l	NOC	14.10	5.47	256.00	5.41
2 10 1987	27.34 139.92	459	4.69	341 38 -76	m	INU	8.37	4.76	213.33	4.71
13 12 1987	30.39 138.09	444	4.03	64 33 -167	m	INU	5.03	4.06	213.33	4.09

Table 1 (continued)

Date D M Y	Epicenter (°N; °E)	Depth (km)	M_m^{mb}	Focal Solution (ϕ, δ, λ)	Ref. †	Station	Δ (°)	M_m	Period (s)	M_c
6 7 1988	-17.68 -178.88	549	4.92	16 53 149	p	NOU	14.61	4.79	213.33	4.74
7 9 1988	30.32 137.37	491	6.01	26 45 166	p	INU	5.03	5.82	213.33	5.77
13 9 1988	29.99 138.47	446	4.92	76 22 -175	p	INU	5.49	4.16	213.33	4.79
16 11 1988	-21.74 -179.52	623	4.76	121 22 166	q	NOU	13.16	5.02	213.33	5.09

† References for published values of M_0 and focal geometry: a: Dziewonski *et al.* (1983*a*); b: Dziewonski *et al.* (1983*b*); c: Dziewonski *et al.* (1985); d: Dziewonski *et al.* (1986*a*); e: Dziewonski *et al.* (1986*b*); f: Dziewonski *et al.* (1987*a*); g: Dziewonski *et al.* (1987*b*); h: Dziewonski *et al.* (1987*c*); i: Dziewonski *et al.* (1987*d*); j: Dziewonski *et al.* (1988*a*); k: Dziewonski *et al.* (1988*b*); l: Dziewonski *et al.* (1988*c*); m: Dziewonski *et al.* (1989*a*); n: Dziewonski *et al.* (1989*b*); o: Dziewonski *et al.* (1989*c*); p: Dziewonski *et al.* (1989*d*); q: Dziewonski *et al.* (1989*e*).

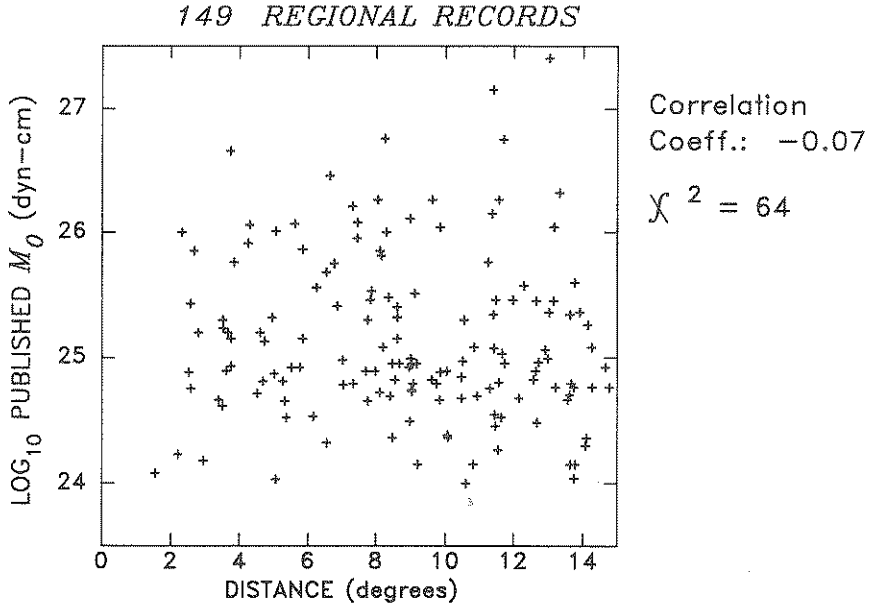

Figure 3
Epicentral distances and published moments for the dataset used in this study. Note the absence of correlation between the two parameters.

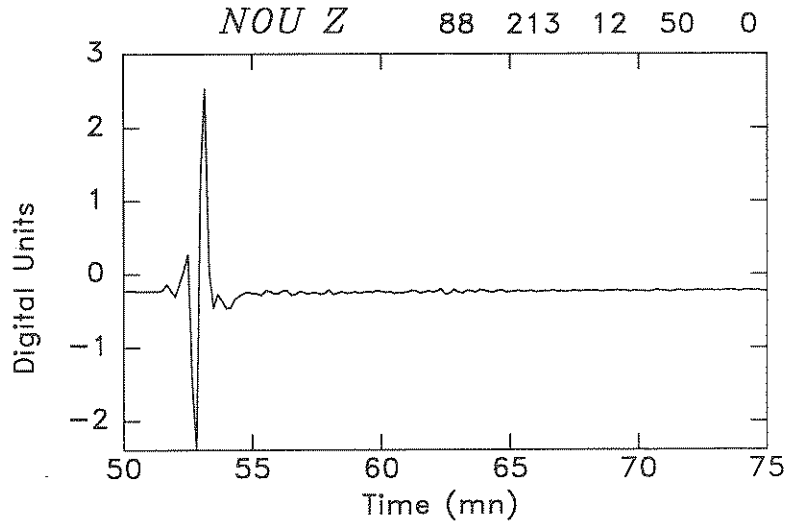

Figure 4
Example of a typical GEOSCOPE record at regional distances (Event of 31 July 1988 recorded at Port Laguerre, New Caledonia ($\Delta = 4.22°$)). This record shows that it is impossible to separate the long-period Rayleigh energy from the body waves. Also, because of insufficient dispersion of the group times, it is no longer possible to make measurements in the time domain.

3. Methodology

The algorithm for the measurement of the mantle magnitude M_m has been described in detail in Paper I. The only problem at short distances is the difficulty of isolating the Rayleigh wave in the record. As exemplified on Figure 4, there is often no alternative but to process the entire seismogram, including the *P*- and *S*-waves; we are justified in doing so by the fact that body waves carry very little energy in the mantle frequency range. The quality of our results provides a further *a posteriori* justification of this procedure.

As discussed more in detail elsewhere (OKAL, 1989), it is no longer possible at short distances to make a direct measurement in the time domain, since sufficient dispersion cannot take place over a short path, and consequently individual frequencies cannot be resolved on the basis of their different group times.

As in the case of teleseismic distances, we define a residual $r = M_m - \log_{10} M_0 + 20$, based on the published value of the moment of the event, and study the population of residuals r. We also address the question of the influence of focal geometry and depth by computing the true excitation E in the published focal and receiver geometry as defined in Equation (8) of Paper I, and a "focal mechanism contribution" $C_{FM} = -\log_{10} E - C_S$. Then $M_c = M_m + C_{FM}$ is the value which would have been computed, had we taken into account the exact depth and

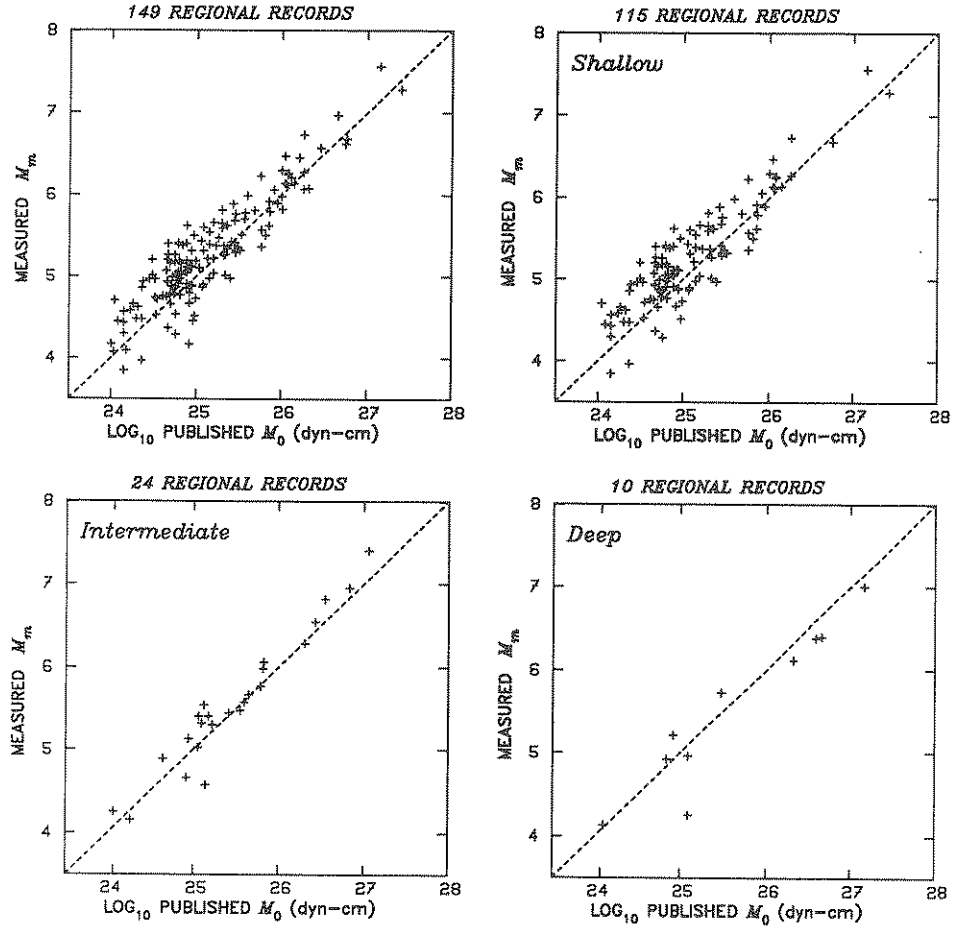

Figure 5

Performance of M_m for the regional dataset. Each diagram plots individual values of M_m, as measured in this study, against values of the moment M_0 of the events, as published in the Harvard CMT solutions (DZIEWONSKI *et al.*, 1983a and subsequent updates). The various boxes refer to the whole dataset (upper left), or to the sub-datasets in the various depth windows. The dashed line is the expected relation: $M_m = \log_{10} M_0 - 20$.

geometry of the event, rather than used the average excitation featured in the correction C_S. We further define the corrected residual $r_c = M_c - \log_{10} M_0 + 20$.

4. Results

Table 1 lists the individual values of M_m for all 149 records comprising the dataset. These values are plotted against the published value of M_0 on Figure 5. It is immediately apparent that the quality of this dataset is generally comparable to

Table 2

Summary of results at regional distances

Dataset	Station Code	Number of Records	$\bar{r}$	σ	Slope	$\bar{r_c}$	σ_c
Whole dataset		149	0.13	0.28	1.01	0.17	0.28
Shallow only		115	0.17	0.29	1.02	0.20	0.30
Intermediate (A and B)		24	0.07	0.19	0.92	0.12	0.16
Deep		10	−0.11	0.27	1.03	−0.02	0.17
For Reference:							
Original Teleseismic Rayleigh dataset[a]		456	0.14	0.24	1.07	0.10	0.18
Teleseismic Love dataset[b]		307	0.12	0.29	0.96	0.19	0.25
4-year dataset of automated measurements[c]		474	0.07	0.22	1.02	0.02	0.27
	Individual stations						
Nouméa, New Caledonia	NOC, NOU*	54	0.06	0.20	1.02	0.20	0.28
Inuyama, Japan	INU	30	−0.03	0.29	0.98	0.03	0.20
Dumont d'Urville, Antarctica	DRV	13	0.42	0.15	1.00	0.16	0.09
Saint-Sauveur de Badole, France	SSB	11	0.09	0.36	0.92	0.20	0.20
Cayenne, French Guiana	CAY	10	0.38	0.13	0.94	0.28	0.11
Santa Cruz, California	SCZ	10	0.16	0.20	1.08	0.29	0.57

* We treat as a single dataset records from the New Caledonia station before and after it was moved (about 20 km) to Port Laguerre (NOU) in March, 1988.

[a] This dataset combines the original records from shallow earthquakes (Paper I), and those from the intermediate and deep study (OKAL, 1990).

[b] From Paper II.

[c] From HYVERNAUD *et al.* (1992).

that of the teleseismic studies in Papers I and II. It can be further assessed along the following lines:

Accuracy of M_m

Statistics regarding the populations r and r_c are given in Table 2. The dataset is considered as a whole or broken down into shallow, intermediate and deep events. Given the small number of records involved, it was not possible to further distinguish between the (A) and (B) families of intermediate earthquakes (OKAL, 1990). In general, the average residuals $\bar{r}$ and standard deviations σ (0.13 and 0.28 respectively for the whole dataset) are comparable to those achieved at teleseismic distances. As shown on Figure 6, however, corrections for focal geometry and depth fail to achieve the same level of variance reduction. In a pattern reminiscent of the teleseismic studies in Paper I, the two very large residuals r_c on Figure 6 correspond to geometries where the station is expected to be strongly nodal for the published focal mechanism, but nevertheless substantial energy is present in the record. At shorter distances, it is less likely that the wave travels outside the great

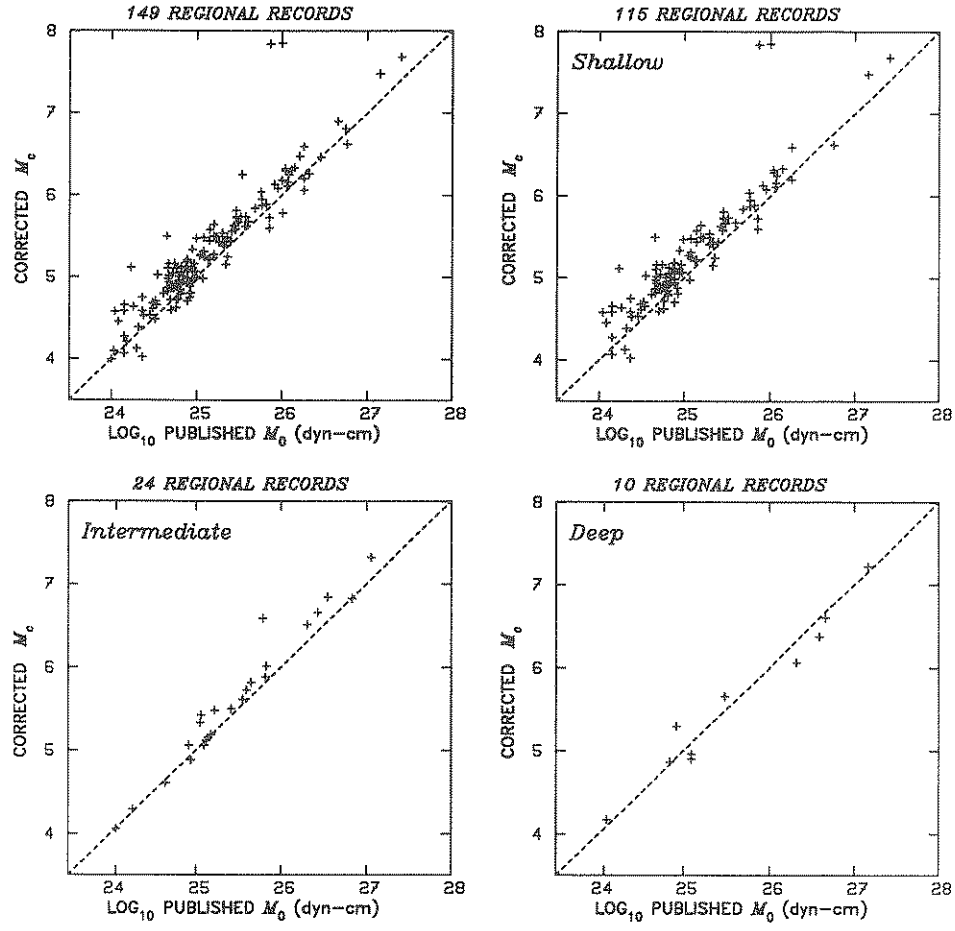

Figure 6
Same as Figure 5 for the "corrected" M_c. Note the slight improvement in the residuals. See text for comment on the two very large residuals in the shallow dataset.

circle due to lateral heterogeneity, but on the other hand, the large values of r_c may reflect the increased inaccuracy of source-to-station azimuths: at very short distances, a small error in either the epicentral location or the focal geometry could result in a significant error in the position of the station with respect to the radiation pattern of Rayleigh waves, and eventually in the focal correction C_{FM} as defined in Paper I. Indeed, under such conditions, the concept of magnitude appears more robust than the use a full-fledged moment tensor.

M_0:M_m Relationships

These can be characterized by the best-fitting slopes regressing the datasets shown on Figure 5. As evident from the 6th column of Table 2, these slopes are not

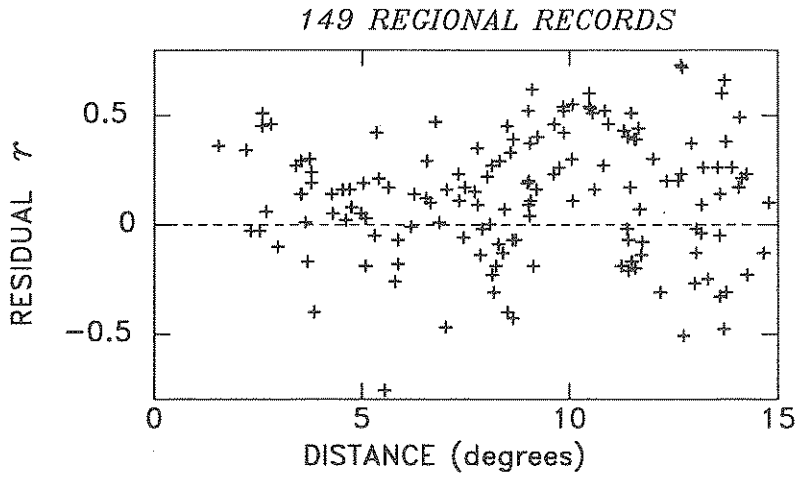

Figure 7
Residuals r plotted as a function of distance (for the whole dataset). The absence of trend with distance confirms that no breakdown in the reliability of M_m can be detected.

significantly different from 1, which proves that the growth of M_m with moment remains linear, and in particular that saturation effects have been effectively prevented. Once again, the slopes are comparable to their teleseismic counterparts.

Behavior with Distance

The most crucial test to be performed on our population of residuals is to explore any possible trend with distance. The onset of systematically positive (or negative) residuals below a certain distance threshold would signal the onset of the breakdown of the asymptotic expansion (2). As shown on Figure 7, no such trend could be found. We further explored the matter by regressing the residual population against distance. The resulting slope is only 0.004 units of magnitude per degree, corresponding to a trend of less than 0.1 unit over the full range of distances, which remains below the typical scatter in the residuals. A statistical analysis of the populations of distances and residuals yields a correlation coefficient of only 0.05, and $\chi^2 = 11.7$, indicating a probability of correlation of less than 1%. An attempt at regressing r against $\log_{10} \Delta$ yields similarly unsignificant trends.

Finally, we studied a restricted dataset consisting of only the records obtained at $\Delta \leq 7°$, with the goal of detecting any possible increase in the scatter of the measurements at very short distances. The average residual ($\bar{r} = 0.09$ and the new standard deviation ($\sigma = 0.25$) are practically unchanged, and if anything, slightly better than for the whole dataset; on the other hand, for the corrected values, $\bar{r}_c = 0.17$ is unchanged, but the standard deviation increases to $\sigma_c = 0.33$, a further

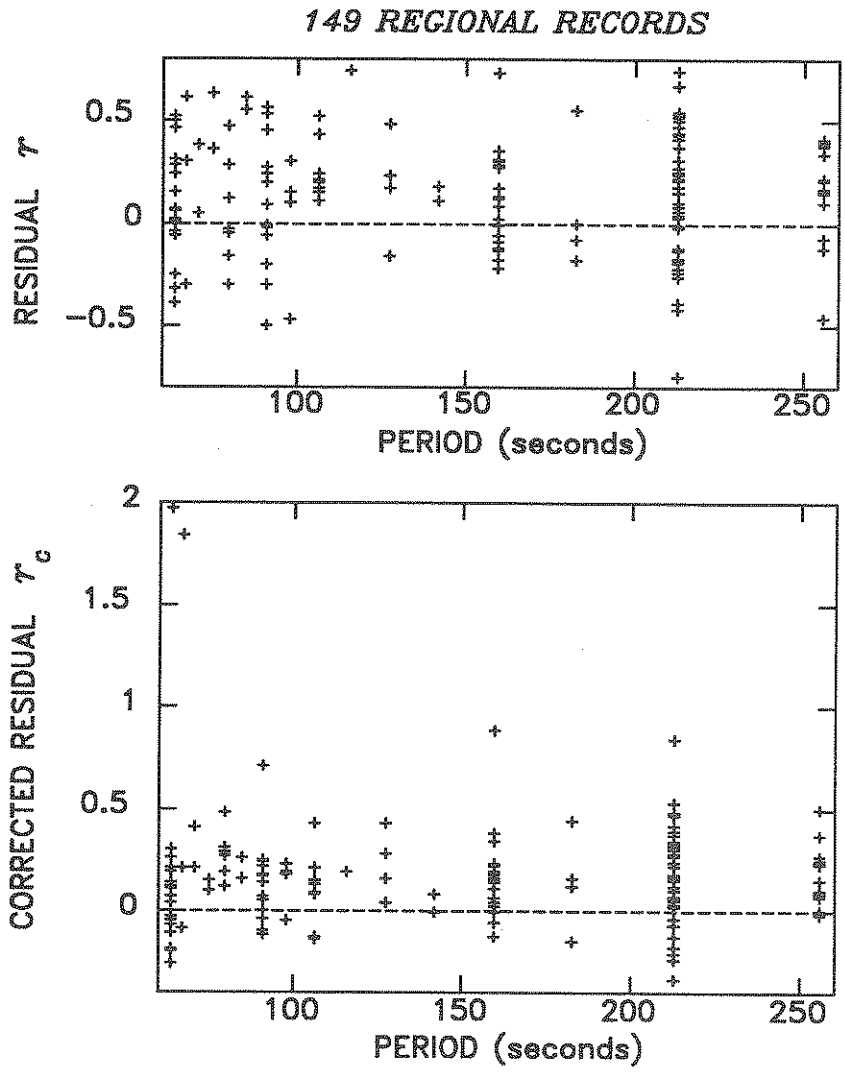

Figure 8
Residuals as function of period. *Top*: Raw residuals r; *Bottom*: Corrected residuals r_c. See text for discussion.

illustration that large corrected residuals r_c are probably due, at least in part, to inaccuracy in the geometry used when computing C_{FM} (see above).

We conclude that we fail to identify in our dataset any evidence of a degradation of the performance of M_m with distance.

Behavior with Period

We next study the residuals r and r_c as a function of the period T at which they were retained. Figure 8 shows that, again, no trend can be identified, the regression

of r vs. $\log_{10} T$ yielding an insignificant slope of 0.029, or 0.01 unit of magnitude per octave. The correlation coefficient was found to be 0.02, with $\chi^2 = 11$. This check was important, since as suggested by Figure 1, the breakdown of the asymptotic expansion of the Legendre polynomials is expected to be wavelength-controlled, and hence period-dependent. As we noted in Paper I in the teleseismic case, the extravagant residuals r_c occur at the shorter periods.

Behavior at Individual Stations

Finally, like in our previous studies, we split the datasets by individual stations (when a station contributed at least 10 records to the dataset). As in the case of

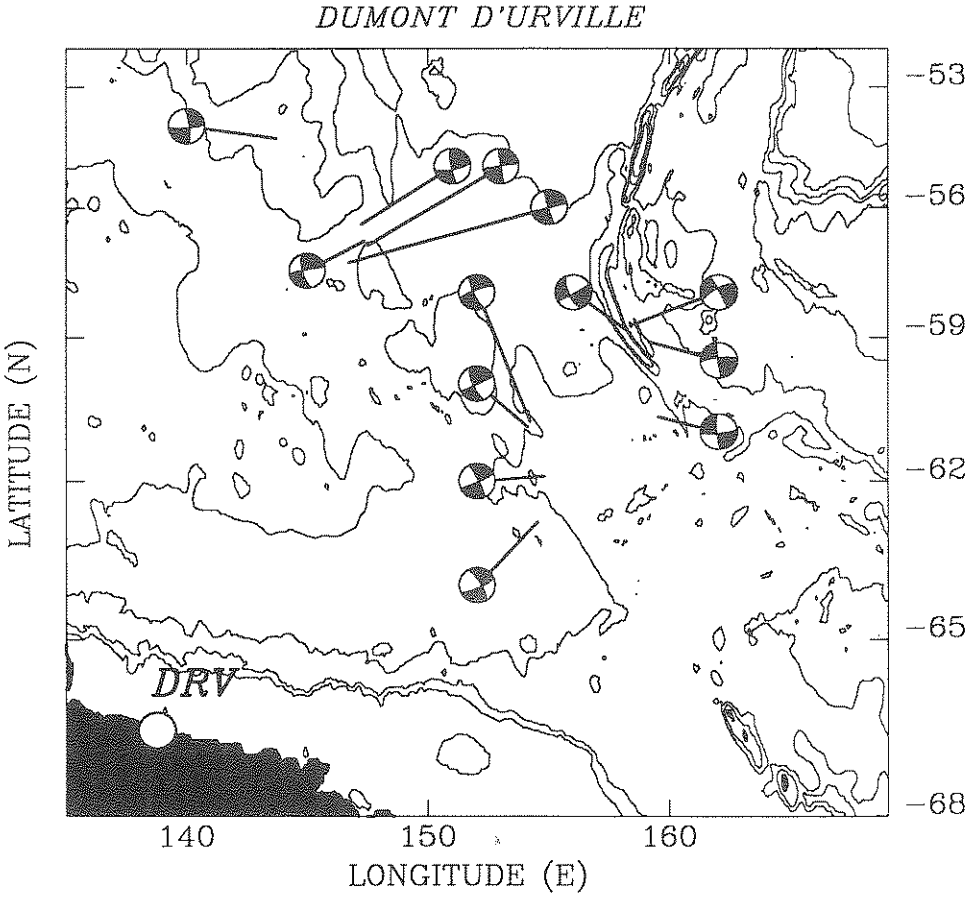

Figure 9

Detailed source-receiver geometry for the dataset at Dumont d'Urville, Antarctica. All earthquakes involve strike-slip rupture in a geometry where DRV sits in a lobe of radiation, giving rise to large residuals r, but much smaller corrected residuals r_c. This is a Mercator projection of the SYNBAPS bathymetry, with isobaths at 1000 m intervals.

teleseismic distances, we were unable to detect any significant trends or station anomalies, suggesting once again that station corrections are not warranted. In the particular case of station DRV, which features a very large average residual ($\bar{r} = 0.42$), all relevant earthquakes are transform fault events, clustered at several locations along the nearby plate boundaries for which DRV sits in a lobe of Rayleigh radiation (Figure 9). The large residuals are an artifact of this geometry, and are all but eliminated when a focal correction is applied, and the residuals r_c considered.

5. Conclusions

The extension of the algorithm for the computation of the mantle magnitude M_m to the field of regional distances is not accompanied by any detectable deterioration of its performance. The population of residuals r from the regional dataset has statistical characteristics (accuracy, standard deviaiton, slope) comparing favorably with those obtained at teleseismic distances. We could not identify any significant trend with variables such as period or distance which would point out to the initiation of the breakdown of the assumptions used in deriving M_m, even for distances as short as 1.5° and periods as long as 256 s.

The validity of the mantle magnitude algorithm in regional distances upholds the concept of using M_m to obtain in real time an estimate of the seismic moment of an event, with important applications in the field of tsunami warning (TALANDIER and OKAL, 1989).

Acknowledgments

We thank Barbara Romanowicz and Jean-Paul Montagner for providing a regular flow of GEOSCOPE data; Göran Ekström sent us updates of the Harvard CMT catalog in advance in publication. We thank Paul Stoddard and Paul Lundgren for developing map-plotting software, and Michael Wysession for the use of his statistical package. This research was supported by Commissariat à l'Energie Atomique (France), and the National Science Foundation, under grant EAR-87-20549.

References

DZIEWONSKI, A. M., FRIEDMAN, A., and WOODHOUSE, J. H. (1983a), *Centroid Moment-tensor Solutions for January–March 1983*, Phys. Earth Planet. Inter. *33*, 71–75.

DZIEWONSKI, A. M., FRANZEN, J. E., and WOODHOUSE, J. H. (1983b), *Centroid Moment-tensor Solutions for April–June 1983*, Phys. Earth Planet. Inter. *33*, 243–249.

DZIEWONSKI, A. M., FRANZEN, J. E., and WOODHOUSE, J. H. (1985), *Centroid Moment-tensor Solutions for April–June 1984*, Phys. Earth Planet. Inter. *37*, 87–96.

DZIEWONSKI, A. M., FRANZEN, J. E., and WOODHOUSE, J. H. (1986a), *Centroid Moment-tensor Solutions for July–September 1985*, Phys. Earth Planet. Inter. *42*, 205–214.

DZIEWONSKI, A. M., FRANZEN, J. E., and WOODHOUSE, J. H. (1986b), *Centroid Moment-tensor Solutions for October–December 1985*, Phys. Earth Planet. Inter. *43*, 185–195.

DZIEWONSKI, A. M., FRANZEN, J. E., and WOODHOUSE, J. H. (1987a), *Centroid Moment-tensor Solutions for January–March 1986*, Phys. Earth Planet. Inter. *45*, 1–10.

DZIEWONSKI, A. M., EKSTRÖM, G., FRANZEN, J. E., and WOODHOUSE, J. H. (1987b), *Centroid Moment-tensor Solutions for April–June 1986*, Phys. Earth Planet. Inter. *45*, 229–239.

DZIEWONSKI, A. M., EKSTRÖM, G., FRANZEN, J. E., and WOODHOUSE, J. H. (1987c), *Centroid Moment-tensor Solutions for July–September 1986*, Phys. Earth Planet. Inter. *46*, 305–315.

DZIEWONSKI, A. M., EKSTRÖM, G., WOODHOUSE, J. H., and ZWART, G. (1987d), *Centroid Moment-tensor Solutions for October–December 1986*, Phys. Earth Planet. Inter. *48*, 5–17.

DZIEWONSKI, A. M., EKSTRÖM, G., WOODHOUSE, J. H., and ZWART, G. (1988a), *Centroid Moment-tensor solutions for January–March 1987*, Phys. Earth Planet. Inter. *50*, 116–126.

DZIEWONSKI, A. M., EKSTRÖM, G., WOODHOUSE, J. H., and ZWART, G. (1988b), *Centroid Moment-tensor Solutions for April–June 1987*, Phys. Earth Planet. Inter. *50*, 215–225.

DZIEWONSKI, A. M., EKSTRÖM, G., WOODHOUSE, J. H., and ZWART, G. (1988c), *Centroid Moment-tensor Solutions for July–September 1987*, Phys. Earth Planet. Inter. *53*, 1–11.

DZIEWONSKI, A. M., EKSTRÖM, G., WOODHOUSE, J. H., and ZWART, G. (1989a), *Centroid Moment-tensor Solutions for October–December, 1987*, Phys. Earth Planet. Inter. *54*, 10–21.

DZIEWONSKI, A. M., EKSTRÖM, G., WOODHOUSE, J. H., and ZWART, G. (1989b), *Centroid Moment-tensor Solutions for January–March, 1988*, Phys. Earth Planet. Inter. *54*, 22–32.

DZIEWONSKI, A. M., EKSTRÖM, G., WOODHOUSE, J. H., and ZWART, G. (1989c), *Centroid Moment-tensor Solutions for April–June, 1988*, Phys. Earth Planet. Inter., *54*, 199–209.

DZIEWONSKI, A. M., EKSTRÖM, G., WOODHOUSE, J. H., and ZWART, G. (1989d), *Centroid Moment-tensor Solutions for July–September 1988*, Phys. Earth Planet. Inter. *56*, 165–180.

DZIEWONSKI, A. M., EKSTRÖM, G., WOODHOUSE, J. H., and ZWART, G. (1989e), *Centroid Moment-tensor Solutions for October–December, 1988*, Phys. Earth Planet. Inter. *57*, 179–191.

HYVERNAUD, O., REYMOND, D., TALANDIER, J., and OKAL, E. A. (1992), *Four Years of Automated Measurement of Seismic Moments at Papeete using the Mantle Magnitude M_m: 1987–1991*, Tectonophys., submitted.

KANAMORI, H., and CIPAR, J. J. (1974), *Focal Process of the Great Chilean Earthquake, May 22, 1960*, Phys. Earth Planet. Inter. *9*, 128–136.

OKAL, E. A. (1989), *A Theoretical Discussion of Time-domain Magnitudes: The Prague Formula for M_s and the Mantle Magnitude M_m*, J. Geophys. Res. *94*, 4194–4204.

OKAL, E. A. (1990), *M_m: A Mantle Wave Magnitude for Intermediate and Deep Earthquakes*, Pure Appl. Geophys. *134*, 333–354.

OKAL, E. A., and TALANDIER, J. (1989), *M_m: A Variable Period Mantle Magnitude*, J. Geophys. Res. *94*, 4169–4193.

OKAL, E. A., and TALANDIER, J. (1990), *M_m: Extension to Love Waves of the Concept of a Variable-period Mantle Magnitude*, Pure Appl. Geophys. *134*, 355–384.

REYMOND, D., HYVERNAUD, O., and TALANDIER, J. (1991), *Automatic Detection, Location and Quantification of Earthquakes: Application to Tsunami Warning*, Pure Appl. Geophys. *135*, 361–382.

TALANDIER, J., and OKAL, E. A. (1989), *An Algorithm for Automated Tsunami Warning in French Polynesia, Based on Mantle Magnitudes*, Bull. Seismol. Soc. Am. *79*, 1177–1193.

(Received January 12, 1992, accepted January 28, 1992)